COMPOSITION GRADIENTS IN SILICATE INCLUSIONS IN CHROMITES FROM THE DUNITIC MANTLE-CRUST TRANSITION (OMAN OPHIOLITE) REVEAL HIGH TEMPERATURE FLUID-MELT-ROCK INTERACTION CONTROLLED BY FAULTING

Mathieu Rospabé*,✉, Georges Ceuleneer, Mathieu Benoit**** and **Mary-Alix Kaczmarek****

** Research Institute for Marine Geodynamics (IMG), Japan Agency for Marine-Earth Science and Technology (JAMSTEC), Yokosuka, Kanagawa, Japan.*

*** Géosciences Environnement Toulouse (GET), Observatoire Midi-Pyrénées, Université de Toulouse, CNRS, IRD, Toulouse, France.*

✉ *Corresponding author, e-mail: mrospabe@jamstec.go.jp*

Keywords: *silicate inclusions; disseminated chromites; variably impregnated dunites; dunitic mantle-crust transition zone; fluid-melt-peridotite interaction; hybridization; Maqsad; Oman ophiolite.*

ABSTRACT

The transition between the mantle section and the oceanic crust in the Maqsad area (Oman ophiolite) is mainly made of variably impregnated dunites locally associated with chromitite ore bodies. There, the dunitic transition zone (DTZ) developed above a mantle diapir that fed with MORB the former oceanic spreading centre. However, orthopyroxene and amphibole impregnations in dunites from the DTZ are witnesses of a hydrated magmatism that looks restricted to this interface. The main other piece of evidence is the nature of silicate minerals included in chromite grains scattered in dunite (e.g., amphibole, orthopyroxene, mica), which are mostly issued from a hydrated and silica-rich melt or fluid. Here, we report on a study of such inclusions along a section sampled in detail in the Maqsad DTZ. It brings critical information on the processes involved in the fluid-melt-peridotite reaction below oceanic spreading centres, complementary to the one provided by the interstitial silicates forming the matrix of the dunite. We first show that both the nature and the composition of the inclusions are well-correlated to those of the impregnations in the host dunites, then that the chemical evolution along the cross-section for all materials correlate to the presence of faults that developed at an early, syn-magmatic stage. This confirms that the early tectonics in the deep oceanic lithosphere primarily controls the fluid-melt-rock reactions and can condition chemical cycling, including for halogens (Cl, F), in oceanic spreading centre setting.

INTRODUCTION

The boundary between the mantle and the oceanic crust is known to be a reactive transition where significant interactions occur between the melts issued from the deep mantle partial melting, whatever their composition, and the peridotites from the uppermost mantle. These processes, called melt-rock reactions, lead to mineral resorption and/or precipitation (i.e. modal metasomatism) as well as to chemical re-equilibration between the migrating melts and the surrounding rocks (i.e. cryptic metasomatism) (e.g., Kelemen, 1990; Kelemen et al., 1995; Constantin, 1999; Godard et al., 2000; Koga et al., 2001; Sanfilippo et al., 2014; 2016; Rospabé et al., 2018), and thus may have a big impact on the chemical and material transfers below oceanic spreading centres in different settings and at various expansion rates. Dunites and chromitites are frequently observed at the mantle-crust transition both in ophiolites and in present-day oceans, and look to be two important petrological products of melt-peridotite reaction. In this context, dunite is mainly interpreted as a former mantle harzburgite modified by interaction with a melt migrating interstitially along grain boundaries: due to the undersaturated-in-silica character of the melt at low pressure, it induces the dissolution of pyroxenes and the concomitant precipitation of olivine, leading to a 'residual', actually reactive, product made of olivine and minor chrome-spinel (Dick, 1977; Quick, 1981; Kelemen, 1990; 1992).

One hypothesis calls for a hydrated environment for this dunitization process below oceanic spreading centres, a melt hybrid between the MORB and a hydrated component enhancing the transformation of the former mantle harzburgite and the melting out of residual orthopyroxene (Rospabé et al., 2017; 2018). Recent studies in the Oman ophiolite highlighted the importance of the development of deep-seated synmagmatic faults, i) for the accretion of the oceanic lithosphere, triggering the deep introduction of seawater that interacted with the magmatic system (Abily et al., 2011) and, ii) on the genesis of such hybrid melts along these avenues for fluids (Rospabé et al., 2019a; 2019b). On the other hand, the presence of hydrous silicate inclusions in chromite grains from Oman and elsewhere is a long-standing observation likewise calling for the hydrated formation environment of chromitites (e.g., Johan et al., 1983; 2017; Talkington et al., 1984; Matveev and Ballhaus, 2002; Borisova et al., 2012). Therefore, it suggests that common fluid-melt hybridization processes, or fluid-melt-peridotite reactions, may account for the formation of both dunites and chromitite beneath oceanic spreading centres.

In the Maqsad area of the Oman ophiolite, the lithosphere accreted in a MORB magmatic environment (Ceuleneer et al., 1996; Benoit et al., 1996; Kelemen et al., 1997; Korenaga and Kelemen, 1997; Koga et al., 2001; Python and Ceuleneer, 2003) and the hydrated features look restricted to the dunitic mantle-crust transition zone (DTZ) (Rospabé et al., 2017; Rospabé, 2018). In this area, the nature and chemical compositions of magmatic impregnations in dunites (i.e. crystallized from interstitial melts percolating between olivine grains) and of silicate inclusions in chromite grains, disseminated at the scale of the whole DTZ or concentrated in chromitite ore bodies, are very akin (Borisova et al., 2012;

Rospabé et al., 2017). However, no study was fully dedicated to the detailed study of such silicate inclusions in chromite grains in a well-established petrological, geochemical and structural frame, while they may provide essential information about the fluid-melt-peridotite reaction at the mantle-crust transition and thus on the relationship between dunite and chromitite.

In this article, we present a detailed description of the silicate inclusions in chromite along a near 400 m-thick cross-section already characterized for its petrology, geochemistry and structural features (Rospabé et al., 2019a). The main purposes of this study are: i) to explore the similarities and/or distinctions between the silicate inclusions in chromite grains disseminated in the DTZ on one hand, and the mineral impregnations partly forming the matrix of the host dunites on the other hand; and ii) to test the hypothesis of the possible influence of the synmagmatic faults on the hybridization of the fluids/melts that have dissolved and fractionated the Cr at the mantle-oceanic crust transition.

GEOLOGICAL BACKGROUND AND SAMPLES

The Oman ophiolite is the largest oceanic lithosphere fragment preserved from the Tethys ocean. It accreted along a possibly fast spreading centre circa 95-97 million years ago contemporaneously, soon before or soon after the initiation of the intra-oceanic thrusting event (Boudier et al., 1988; Montigny et al., 1988; Warren et al., 2005; Rioux et al., 2013; 2016) that preceded its final obduction onto the Arabian margin ~ 70 Ma ago (Glennie et al., 1973). At the scale of the ophiolite, the spatial distribution of the petrological nature of, i) mafic dikes cross cutting the harzburgitic mantle section and, ii) cumulates from the lower crustal section, attests to the coexistence of both MORB and depleted calc-alkaline series at the time of the igneous accretion of the ophiolite (Benoit et al., 1999; Python and Ceuleneer, 2003; Python et al., 2008; Clénet et al., 2010; Abily, 2011).

The largest MORB segment is located in the SE of the ophiolite (Python and Ceuleneer, 2003; Python et al., 2008). It was centred on and fed with melts by a mantle uprising structure now frozen in the Sumail massif (evidenced by the high-temperature plastic deformation pattern recorded in harzburgites) and known as the Maqsad diapir (Rabinowicz et al., 1987; Ceuleneer et al., 1988; Ceuleneer, 1991; Jousselin et al., 1998). The strong igneous activity related to the rise of the Maqsad diapir is attested by: i) abundant melt migration structures cropping out within the residual, harzburgitic mantle section (Ceuleneer et al., 1996; Benoit et al., 1996; Python and Ceuleneer, 2003); ii) the thick dunitic mantle-crust transition zone (DTZ) especially atop the diapiric structure (> 300 m) (Ceuleneer and Nicolas, 1985; Boudier and Nicolas, 1995; Jousselin et al., 1998; Abily and Ceuleneer, 2013; Rospabé, 2018); and iii) numerous chromitite ore bodies observed in both the DTZ and the mantle section (in this case systematically surrounded by a dunitic aureole) (Ceuleneer and Nicolas, 1985).

The dunites from the Maqsad DTZ are mainly interpreted as a reactional product of melt-peridotite interactions in the uppermost harzburgitic mantle (i.e. orthopyroxene resorption) (e.g., Boudier and Nicolas, 1995; Godard et al., 2000; Koga et al., 2001; Rospabé et al., 2018). However, a double origin cannot be ruled out since the uppermost few tens of meters of the DTZ (i.e. approaching the base of the lower gabbroic crust) have a composition consistent with a cumulative origin after olivine fractionation from a Mg-rich melt (Abily and Ceuleneer, 2013). In addition to olivine, the dunites contain a large variety of interstitial minerals considered as impregnation, i.e. that crystallized from an interstitial melt (Rabinowicz et al., 1987; Benn et al., 1988; Boudier and Nicolas, 1995; Koga et al., 2001; Abily and Ceuleneer, 2013; Rospabé et al., 2017; 2018; 2019a).

Clinopyroxene and plagioclase are the most abundant impregnation minerals which are consistent with the MORB igneous environment characterizing the Maqsad area. However, the discovery of interstitial orthopyroxene and amphibole in dunites in the upper half of the DTZ mainly, while virtually absent from the mantle and crustal cumulates in this area, contributed to the development of the hypothesis of a hydrated origin of the DTZ dunites, involving fluid(s) and/or melt(s) richer in silica than the MORB (Rospabé et al., 2017). In this frame, the mantle-crust transition zone may be the place for hybridization between the MORB issued from the deep partial melting within the Maqsad diapir and a downgoing hydrated component - probably hydrothermal seawater in origin. In addition to the peculiar impregnating minerals, another witness of the hydrated magmatism environment in which both dunites and chromitites formed is the frequent presence of hydrous silicate minerals in inclusion in chromite (amphibole, mica among others) observed both in chromitite ore bodies and in chromite grain scattered in dunites (Lorand and Ceuleneer, 1989; Leblanc and Ceuleneer, 1991; Schiano et al., 1997; Borisova et al., 2012; Rospabé et al., 2017; 2019b; Rollinson et al., 2018; Zagrtdenov et al., 2018; Yao et al., 2020) .

Furthermore, the correlation between the vertical chemical patterns across the DTZ dunites and chromitites (whole rocks, matrix minerals) and the presence of fault zones and/or magmatic breccias evidenced that the mantle-crust transition has been tectonically affected at an early magmatic stage, with limited offsets, and that such faults may have favoured the hybridization process (Rospabé et al., 2019a; 2019b; see also Abily et al., 2011). Other recent studies likewise evidenced that chromitites are regularly located along or near faults or shear zones in the Oman ophiolite (Boudier and Al-Rajhi, 2014; Zagrtdenov et al., 2018). All these observations allow pointing out the importance of the structural control on the igneous processes involved in the formation of both dunite and chromitite at the mantle-crust transition beneath oceanic spreading centres, at least in the context of Oman. However, the silicate inclusions in the dispersed chromite grains, ubiquitous in the DTZ dunites, are regularly a left-over of the fluid-melt-rock reaction products, petrologists more commonly studying the dunite matrix or the most spectacular chromitite ore bodies.

In order to better explore the similarities and/or differences in the nature of the silicate inclusions in the scattered chromite grains and the impregnations in the surrounding matrix, and to investigate the role of the early synmagmatic faults on the nature and chemistry of such inclusions, we performed a detailed and systematic determination of the nature and composition of inclusions in chromite in 42 variably impregnated dunites. The samples were collected along a full cross-section that has already been described in terms of major and trace mineral and whole rock compositions as well as for its structural features (cross-section #3 in Rospabé et al., 2019a). The sampling sites extent from 685 to 1072 m in altitude, covering a large portion of the DTZ in this area. It is worth noting that, as the central part of (and above) the Maqsad diapir has escaped from off-axis transposition and that the Sumail mas-

sif is tilted by less than 10°, we consider the current altitudes as close to paleo-depths. The cross-section shows a clear petrological dichotomy that is quite characteristic of the Maqsad DTZ (Rospabé, 2018): i) the half lower part is primarily made of pure dunites (i.e. only olivine and chromite) and of very minor cpx- and amph-bearing dunites, and locally hosts one chromitite (16OM38B, 748 m) and schlierens of chromite (16OM41B and 41C, 772 m); ii) the half upper part, basically above the altitude 850 m, is extensively impregnated with clinopyroxene, plagioclase, amphibole and orthopyroxene, allowing to describe samples as cpx-bearing-, pl-bearing-, cpx/pl-bearing-, opx/pl/cpx-bearing- and amph-bearing (± opx/pl/cpx) dunites (Rospabé et al., 2018) (Fig. 1a).

Three main regional faults and four other minor fractures cross-cut the cross-section, sometimes corresponding to a change in the lithology from pure to impregnated dunites. These structural features were interpreted as synmagmatic faults that later evolved into hydrothermal faults (higher serpentinization degree along fault and fracture planes). They developed early before the end of the igneous activity in this area and influenced both the petrological and geochemical variability of the DTZ (Rospabé et al., 2019a). The faults present two main orientations: N130°E, parallel to the strike of the sheeted dike complex in the Sumail massif (Pallister, 1981; MacLeod and Rothery, 1992), i.e. parallel to the paleo-ridge axis and to the MORB segment fed by the Maqsad diapir (Ceuleneer, 1991; Python and Ceuleneer, 2003) - and N165°E to N180°E, parallel to the high temperature Muqbariah shear zone limiting to the SW the area fed by mantle flux diverging from the diapir (Amri et al., 1996).

DISTRIBUTION OF SILICATE INCLUSIONS ACROSS THE DTZ

The nature of the silicate inclusions in chromite has been determined according to their microprobe analysis. We identified amphibole (amph), clinopyroxene (cpx), diopside of different composition than cpx (diop; see Rospabé et al., 2017 and the description of chemistry below), mica, orthopyroxene (opx) and olivine (ol) as the major mineral phases in inclusions. They have all been observed both as monomineralic inclusions or as parts of polymineralic inclusions indifferently. Amphibole and clinopyroxene are by far the most abundant minerals in inclusion in the disseminated chromites in samples from this cross-section (Fig. 1b), representing more than 80% of all the analyses. As minor contents, we also identified anorthitic plagioclase feldspar (pl), garnet (gt), as well as a more albitic plagioclase (alb) and one chlorapatite (Cl-ap).

We observe the following distribution across the section (Fig. 1):

- The very base - below the lower main fault (< ~ 715 m) - is one of the levels displaying the lesser abundance of inclusions along the cross-section (less than 10 inclusions per thin section) (Fig. 1c). We can observe a little abundance of monomineralic inclusions (at least apparently in thin section) in the chromites dispersed in pure dunites, made of clinopyroxene, by far the most abundant phase (76%), amphibole (22%) and diopside (2%) (Figs. 1b and 2a-b). Polymineralic inclusions are globally absent apart from one assemblage clinopyroxene-mica.

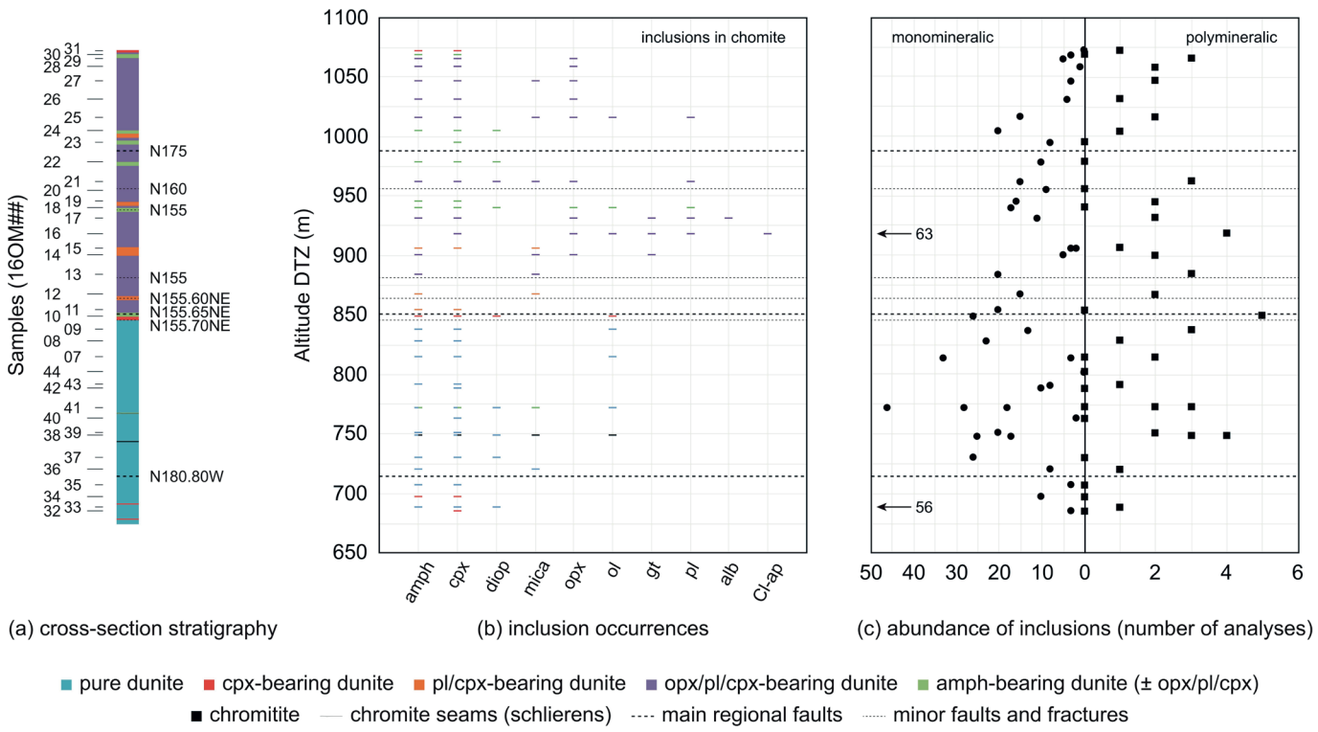

Fig. 1 - Vertical distribution of the silicate inclusions in chromite along the studied cross-section. (a) Petrological and structural log of the cross-section (#3 in Rospabé et al., 2019a). (b) Vertical distribution of the nature of the inclusions in chromite. (c) Vertical distribution of the abundance of these inclusions depending they are mono- or polymineralic. The main regional faults and minor fractures are drawn at the altitude they cut across the cross-section on the field. Abbreviations: amph- amphibole; Cl-ap- chlorapatite; cpx- clinopyroxene; diop- diopside; gt- grossular garnet; ol- olivine; opx- orthopyroxene; pl- plagioclase feldspar.

- The pure dunitic interval in between the lower and the intermediate main faults (~ 715-850 m) also contains mica and olivine in inclusion in addition to amph, cpx and diop, especially near the chromite-rich level around 750 to 775 m in altitude (chromitite, schlierens) (Fig. 1a-b and 2c). This latter interval is also characterized by an increase of the amount of inclusions, both monomineralic and polymineralic. This increase is progressive from levels poor in inclusions to this richer level (Fig. 1c). Monomineralic inclusions are mainly clinopyroxene (57%) then amphibole (34%) (others 9%). Polymineralic inclusions are mainly represented by the association amphibole-clinopyroxene and to a lesser extent by amphibole-diopside and amphibole-mica assemblages.
- The lower impregnated portion, in between the intermediate and the higher main faults (~ 850-990 m), shows the broader variety in included minerals (Fig. 1b). Mica occurs from 867 to 906 m, while this interval is also characterized by the absence of clinopyroxene in inclusion (gap between 854 and 906 m). In addition to amph, cpx, diop, mica and ol, the presence of opx (Fig. 2d-e), gt, pl as well as of one albitic plagioclase and one chlorapatite is attested, especially within the altitude range ~ 900-975 m. The albitic plagioclase was observed in association with anorthitic plagioclase within a polymineralic inclusion (Fig. 2f). The Cl-apatite is associated to orthopyroxene, amphibole partly altered into tremolite, serpentine (derived from opx alteration) and Fe-Ni sulphides (Fig. 2g). In these opx/pl/cpx-bearing- and amph-bearing (± opx/pl/cpx) dunites from the lower impregnated portion, the amount of monomineralic inclusions in chromite grains show alternating decreasing and increasing trends vertically, with a characteristic thickness of about 50 m (Fig. 1c). The higher amounts basically correlate to the intermediate main fault (~ 850 m) and to another minor fracture (~ 955 m). Along this portion, monomineralic inclusions are mainly amphibole, by far (49%), then clinopyroxene (12%) and orthopyroxene (6%) (others 33%). Numerous garnet and plagioclase inclusions were analysed but almost all of them occur in a single sample (16OM16A, 918 m), that contains also the Cl-apatite and a significant proportion of orthopyroxene inclusions. Polymineralic inclusions are mainly made of amphibole-mica and amphibole-clinopyroxene and of a few amphibole-orthopyroxene assemblages along the lower impregnated portion (Fig. 2h).
- The upper impregnated portion, above the higher main fault (> ~ 990 m), corresponds to the altitude level hosting a neighbouring stratiform chromitite ore body (Ceuleneer and Nicolas, 1985; Borisova et al., 2012; Rollinson and Adetunji, 2013; Rospabé et al., 2019b). The inclusion content decreases upsection along this upper part of the section (Fig. 1c). Monomineralic inclusions are mainly clinopyroxene (54%) and amphibole (38%), together with a few orthopyroxene (4%) (others 5%), while polymineralic inclusions are by decreasing order of occurrence amphibole-orthopyroxene, amphibole-clinopyroxene and amphibole-mica assemblages.

At the scale of the entire cross-section, beyond the alternating increases/decreases in the abundance of inclusions, we observe a global decrease in the amount of inclusions (especially the monomineralic ones) from the pure dunitic lower half of the cross-section, especially from the chromite-rich interval, to its impregnated top (i.e. 'Christmas tree-shape' pattern of the vertical distribution of inclusions) (Fig. 1c).

MINERAL CHEMISTRY

Analytical note

The major and minor element content of silicate inclusions and of their host chromite was measured *in situ* by electron probe microanalysis (EPMA), using a Cameca SX 100 (Microsonde Ouest, Brest, France) (accelerating voltage: 15 kV; beam current: 20 nA; electron beam diameter: 1 μm for all analyses; analysis counting time for each type of minerals: 10 s on peak for each element, 5 s on backgrounds on both sides of the peak). Compositions, averaged per sample for each mineral phase in inclusion, are reported in Supplementary Tables 1S-6S.

Host chromite

Dispersed chromites in dunites display variable compositions with XCr ($100 \times Cr/(Cr + Al)$) = 45.6-63.1 mol%, XMg ($100 \times Mg/(Mg + Fe^{2+})$) = 32.8-63.7 mol%, YFe^{3+} ($100 \times Fe^{3+}/(Cr + Al + Fe^{3+})$) = 4.50-16.4 mol%, and TiO_2 = 0.31-1.37 wt% (Rospabé et al., 2019a). The studied chromitite (16OM38B) has chromite with XCr = 58.4 mol%, XMg = 65.7 mol%, YFe^{3+} = 5.77 mol% and TiO_2 = 0.46 wt%.

Amphibole inclusions (Table 1S)

Amphibole inclusions in the dispersed chromites are pargasites to pargasitic hornblendes (~ 2/3) and magnesio-hastingsites to magnesio-hastingsitic hornblendes (~ 1/3) with no preferential distribution in regard to the host dunite type. They are characterized by XMg = 86.1-92.7 mol%, Al_2O_3 = 10.2-14.6 wt%, Cr_2O_3 = 1.76-3.32 wt% and TiO_2 = 0.59-4.71 wt%. The composition of amphibole spans the same variation ranges whatever it occurs as monomineralic inclusions or as parts of polymineralic inclusions (Fig. 3a) and does not show systematic variations relative to the modal content of chromite in the host dunites (Fig. 3b). The Na_2O and K_2O contents vary from 2.85 to 4.07 wt% and from detection limits to 0.93 wt% respectively, defining a XNa ($100 \times Na/(Na + K)$) comprised between 86.2 and 99.8 mol%. The P_2O_5, Cl and F contents were also determined and show variations from detection limits to 0.12 wt%, 0.12 wt%, and 0.17 wt% in average respectively (maximum values obtained for individual analyses: P_2O_5 = 0.30 wt%, Cl = 0.24 wt%, F = 0.40 wt%). The analysed chromitite contains pargasitic hornblende inclusions with XMg = 93.8 mol%, Al_2O_3 = 11.1 wt%, Cr_2O_3 = 3.08 wt%, TiO_2 = 1.50 wt% and XNa = 99.2 mol% (Na_2O = 4.56 wt%).

Clinopyroxene - diopside inclusions (Table 2S)

According to our previous classification (Rospabé et al., 2017), the distinction was made between the composition of 'clinopyroxene', akin from the one of poikilitic magmatic impregnations studied in previous works (e.g., Koga et al., 2001), and the composition of 'diopside' which is intermediate between the visibly igneous cpx and hydrothermal diopside (e.g., in diopsidites from the mantle section; Python et al., 2007a; 2007b; 2011).

Clinopyroxene in inclusion in dispersed chromites is characterized by XMg = 88.3-93.8 mol%, Al_2O_3 = 1.60-3.08 wt%, Cr_2O_3 = 0.93-1.96 wt%, Na_2O = 0.24-0.93 wt% and TiO_2 = 0.15-0.62 wt%, with compositions similar in monomineralic *vs*. polymineralic inclusions and independent from the chromite content in host dunites (Fig. 3c-d). The only one clinopyroxene inclusion analysed in the chromitite has a higher XMg (94.3 mol%) and displays Al_2O_3 = 2.16 wt%, Cr_2O_3 = 1.50 wt%, Na_2O = 1.15 wt% and TiO_2 = 0.29 wt%.

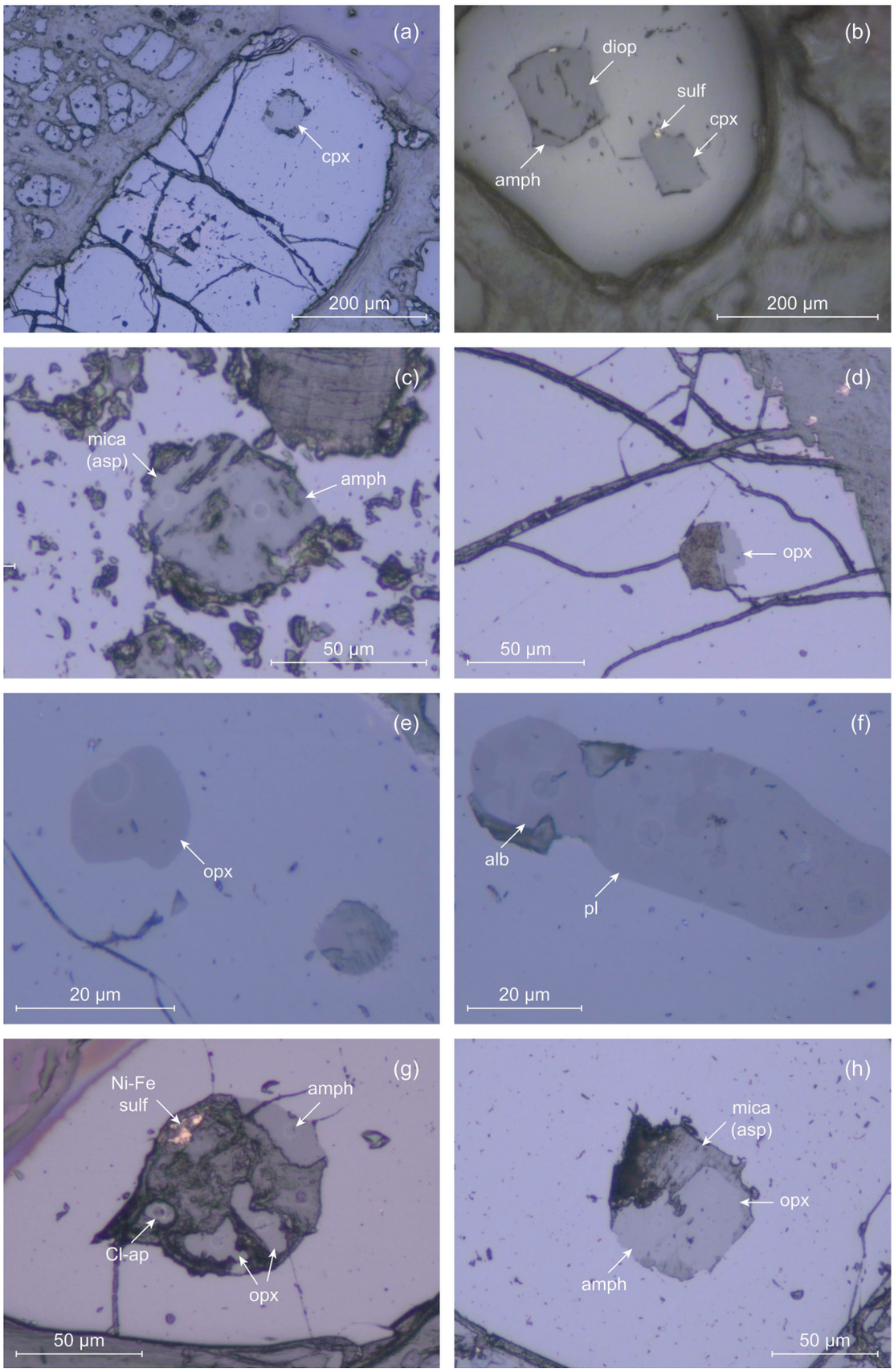

Fig. 2 - Photomicrographs (reflected light) of a few examples of inclusions in disseminated chromites in dunites from the Maqsad DTZ: (a) 16OM07B; (b) 16OM41A: (c) 16OM38; (d) 16OM27; (e) 16OM20; (f) 16OM17; (g) 16OM16A; (h) 16OM14. Abbreviations: alb- albitic plagioclase feldspar; amph- amphibole; asp- aspidolite mica; Cl-ap- chlorapatite; cpx-clinopyroxene; diop- diopside; gt- grossular garnet; ol- olivine; opx- orthopyroxene; phl- phlogopite mica; pl- plagioclase feldspar; sulf- sulphide.

The second type of clinopyroxene called ‘diopside’ was identified in a lesser extent in a few disseminated chromites and is characterized by averaged higher XMg (95.2 mol%) and lower Al_2O_3 (0.70 wt%), Cr_2O_3 (0.78 wt%), Na_2O (0.20 wt%) and TiO_2 (0.13 wt%).

Mica inclusions (Table 3S)

Mica in inclusion in dispersed chromites shows averaged compositions evolving from aspidolite (Na-phlogopite) to intermediate between aspidolite and phlogopite, with a XNa comprised between 37.6 and 98.3 mol% (Na_2O = 2.51-6.79 wt%; K_2O = 0.17-5.45 wt%; $Na_2O + K_2O$ = 4.69-7.97 wt%), but individual analyses of both monomineralic and polymin-

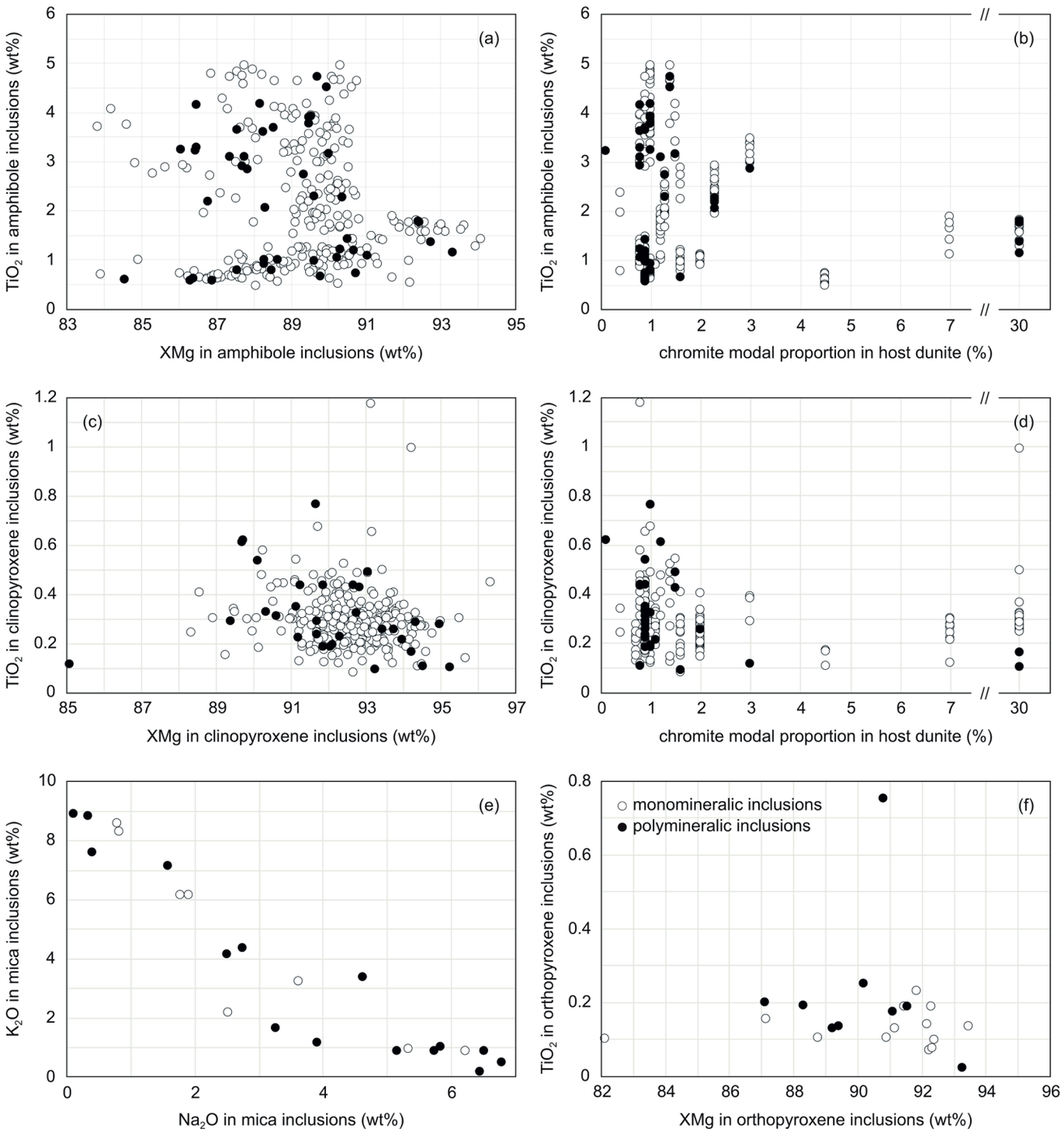

Fig. 3 - Major and minor element compositions of the main chromite-hosted silicate inclusions (individual analyses). Are represented the TiO_2 content as a function of the XMg (100 × molar Mg/(Mg + Fe^{2+}) in amphibole (a), clinopyroxene (c), and orthopyroxene (f), and as a function of the modal content of chromite in the host chromite for amphibole (b), and clinopyroxene (d), as well as the K_2O content as a function of the Na_2O content in mica (e). The distinction is made between the monomineralic inclusions (white circles) and the phases being parts of polymineralic inclusions (black circles).

eralic inclusions span the entire range between the two end-members (Fig. 3e). They are also characterized by a XMg = 90.1-94.5 wt% and by a Ti- and Cr-rich character (TiO_2 = 0.73-5.06 wt%; Cr_2O_3 = 1.60-3.75 wt%). Mica inclusions in the chromitite are characterized by higher XMg (96.7 mol%) and lower TiO_2 (1.46 wt%) averaged values. According to individual analyses, aspidolite is distinguishable from phlogopite in terms of Na_2O (5.33-6.52 wt% *vs*. 0.35-1.90 wt%) and K_2O (0.85-0.94 wt% *vs*. 6.14-8.81 wt%) contents, responsible of two populations in XNa in this chromitite (5.6-32.0 *vs*. 89.6-92.1 mol%, mean 39.3 mol%).

Orthopyroxene inclusions (Table 4S)

Orthopyroxene in inclusion in dispersed chromites is enstatite with XMg = 85.7-93.5 mol%, Al_2O_3 = 0.61-2.76 wt%, Cr_2O_3 = 0.47-1.54 and TiO_2 = 0.02-0.75 wt%. As amphibole and clinopyroxene, orthopyroxene inclusions display similar compositions whatever the mode of occurrence (monomineralic and polymineralic).

Olivine inclusions (Table 5S)

Olivine in inclusion in dispersed chromites is forsterite, characterized by Fo ($100 \times Mg/(Mg + Fe_{total})$) = 88.7-94.8 mol%, NiO = 0.25-0.44 wt% and CaO = 0.02-0.16 wt%. Olivine in inclusion in the chromitite has a high Fo (94.7 mol%) and NiO (0.53 wt%) contents.

Other minor inclusions (Table 6S)

Plagioclase in inclusion is anorthite, with An ($100 \times Ca/(Ca + Na + K)$) = 86.7-90.3 mol%. The albitic, Na-rich plagioclase is characterized by an An content of 33.7 mol%.

Garnet in inclusion is grossular to hydrogrossular with a SiO_2 content (22.2-39.0 wt%) strictly decreasing with the sum of oxides (R^2 = 0.9806) and CaO = 31.3-40.9 wt%, Al_2O_3 = 15.0-24.2 wt% and FeO = 0.58-10.0 wt%.

The Cl-rich apatite is characterized by CaO = 53.3 wt%, P_2O_5 = 41.9 wt%, Cl = 5.39 wt% and F = 0.68 wt%.

Chemical evolutions along the cross-section

The major element composition of chromite and of silicate inclusions shows pronounced variations along the studied cross-section, and defines distinct trends (Fig. 4). Some chemical contents/indexes vary according to the nature of host rocks, especially concerning the composition of chromite and the TiO_2 content in inclusions. For instance, in pure dunites, the TiO_2 content remains mainly below 0.5 wt% in chromite and below 1.5 wt% in amphibole inclusions, while in impregnated dunites it reaches values up to 1.25 wt% in chromite and 4.75 wt% in amphibole (Fig. 4a-b).

The composition of both chromite and silicate inclusions strongly correlates to each other. These variations are not randomly distributed relative to the main regional faults that affect the cross-section, as was already noted for the composition of whole rocks and minerals from the matrix and suspected for the inclusions (Rospabé et al., 2019a). Compositions are evolving continuously on tens of meters toward fault zones rather than showing sudden shifts in their immediate vicinity:

- In the pure dunitic lower part, the increase of XMg in chromite is observed approaching the main faults while the XCr in chromite, XMg and TiO_2 and F contents in amphibole, and Na_2O content in clinopyroxene decrease concomitantly (Fig. 4a-c).
- In the impregnated upper part, the approach of the main faults is marked by an increase of the Cl content in amphibole inclusions associated to the decrease of XNa in amphibole and in a lesser extent mica (i.e. increase of K_2O content relative to the Na_2O content) and of the TiO_2 content in chromite and all silicate inclusions (Fig. 4a-f). These variations are strongest in the vicinity of the upper main fault with a clear common increase of the P_2O_5 and the F contents in amphibole, together with the strongest increase in the Cl content (Fig. 4b). In the upper section above the upper main fault and the altitude of 1000 m, the YFe^{3+} increases drastically and is associated to a decrease in Cr_2O_3 and Al_2O_3 contents in chromite (Fig. 4a).

DISCUSSION

Inclusions in chromite: trapped melts or trapped minerals?

There is no consensus about the very origin of the silicate phases included in chromite. The fact that disseminated chromites in pure dunites, i.e. devoid of any impregnation, contain inclusions likewise prevent for the hypothesis of a 'secondary' origin of the inclusions by melt infiltration through cracks and *in situ* crystallization, and show they were entrapped at the time of the chromite growth. According to some authors, and in the case of the Maqsad DTZ, those present in chromite from chromitites are former trapped melts (i.e. crystallized *in situ* after their entrapment) (e.g., Schiano et al., 1997; Rollinson et al., 2018; Yao et al., 2020). Other authors argue that they are microcrystals already formed in the parent melt or magma at the time they were entrapped (e.g., Borisova et al., 2012; Rospabé et al., 2019b). The homogenization experiments reported in Borisova et al. (2012) have shown that the bulk chemical composition of most inclusions was unlikely the one of any documented natural melt (see also Arai, 1998).

Chromites disseminated in the pure dunite of the lower part of the DTZ contain mostly amphibole and clinopyroxene, mica and diopside inclusions being rather restricted to the chromitite and schlierens. Disseminated chromites in the upper impregnated opx/pl/cpx-bearing- and amph-bearing (± opx/pl/cpx) dunites contain a much diversified mineral content in their inclusions, with in addition to orthopyroxene, plagioclase (mainly anorthitic but one albitic), the more exotic garnet and chlorapatite, as well as most of the mica inclusions (Fig. 1b).

The interstitial minerals between dunite olivine grains are clearly cumulate minerals crystallized from the last melts that percolated through the mantle-crust transition zone in response to the cooling of the system (Rabinowicz et al., 1987; Benn et al., 1988; Boudier and Nicolas, 1995; Koga et al., 2001; Abily and Ceuleneer, 2013; Rospabé et al., 2017; 2018). In the present case, the interstitial orthopyroxene and amphibole were considered as the crystallization product of a lithospheric melt formed at the crust-mantle transition, hybrid between the dry (or water-poor) MORB issued from partial melting within the Maqsad diapir (Ceuleneer et al., 1996; Benoit et al., 1996; Python and Ceuleneer, 2003) and a hydrated component probably deriving from the deep introduction of seawater or hydrothermal fluids (Rospabé et al., 2017). The correlation between the appearance of such mineral impregnations and the change in the nature of the silicate inclusions in chromite in the higher level of the DTZ, especially the common occurrence of orthopyroxene, suggests than both impregnations and silicate inclusions crystallized from melts sharing common characters, possibly from the same Si-, Na-, trace elements-, and volatile-rich hybrid melt.

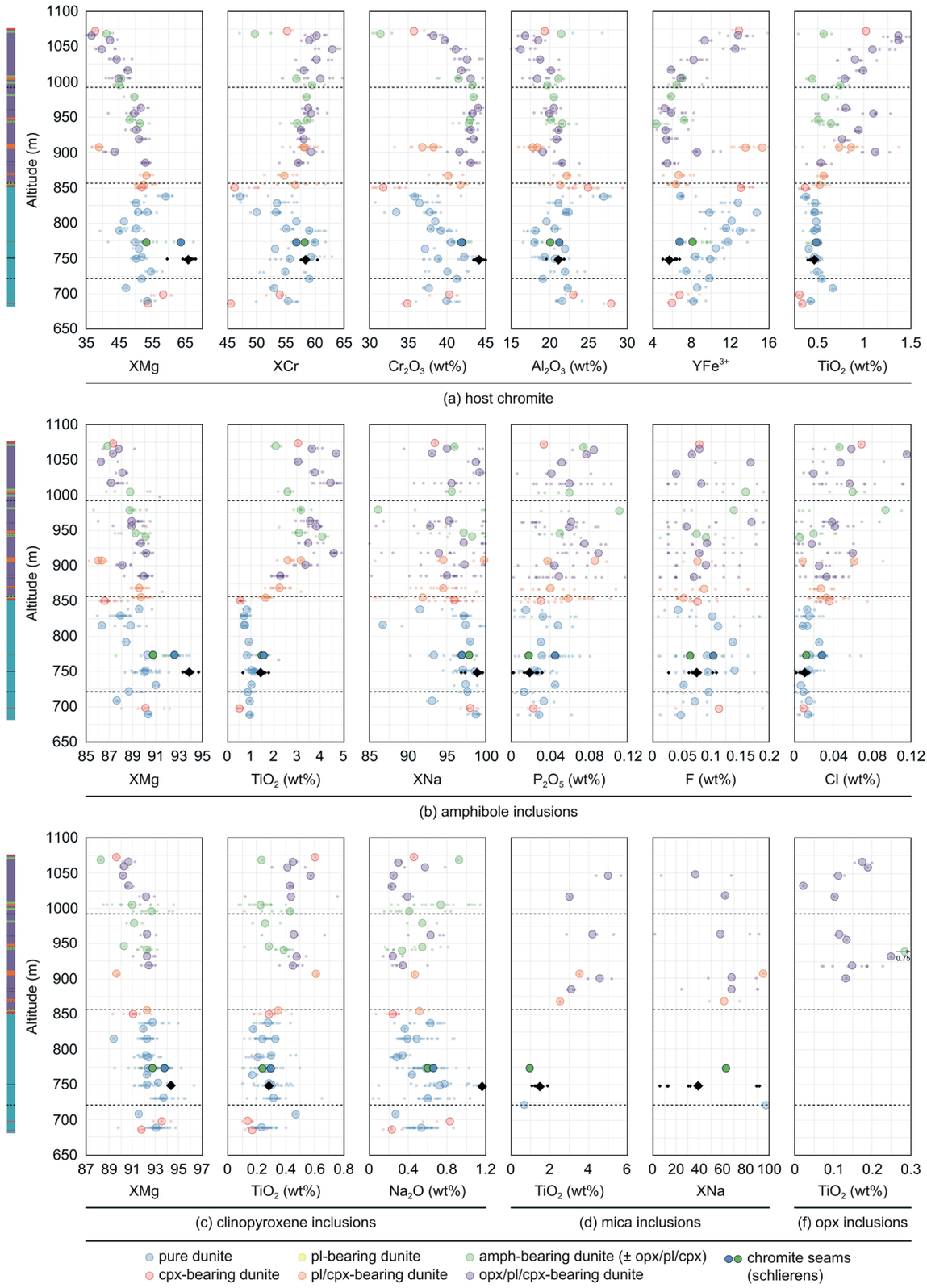

Fig. 4 - Vertical evolution of the major and minor element compositions of disseminated chromite and chromite-hosted silicate inclusions along the cross-section, plotted as a function of the altitude. Are represented, (a) the XMg, XCr, YFe^{3+} and Cr_2O_3, Al_2O_3, TiO_2 contents in chromite, (b) the XMg, XNa and TiO_2, P_2O_5, F and Cl contents in amphibole, (c) the XMg and TiO_2 and Na_2O contents in clinopyroxene, (d) the TiO_2 and XNa in mica and, (e) the TiO_2 content in orthopyroxene. For a given mineral, both averaged values in each sample (bigger dots) and individual analyses (smaller dots) are plotted. Note that these averaged inclusion compositions (calculated from both monomineralic and polymineralic inclusions) partly correlate to the one of host chromites, highlighting that, in a given sample, there is no systematic differences in the composition of a same phase occurring as a monomineralic inclusion or in association with other phases in polymineralic inclusions as deduced from Fig. 3. Averaged values are given in Supplementary Tables 1S-6S. The petrological and structural log described in Fig, 1 is shown to the left of the figure. The main faults observed on the field are also reported in each diagram as the black dotted lines.

Another observation is the clear predominance of monomineralic inclusions relative to polymineralic ones along the cross-section (Fig. 1c). It is more likely explained by the entrapment of tiny crystals rather than by a trapped melt as the complete crystallization of a melt into a single phase must be clearly excluded. As stressed by Rollinson et al. (2018), the surface of an inclusion in a thin section is not representative, and the higher frequency of monomineralic inclusions may be overestimated as it can partly result from the two-dimensional nature of the thin sections, limiting the access to other companion phases in presence in a given 3-D structure. However, would it be the case, it seems unlikely that 90% of the inclusions observed in thin section would appear monomineralic. This statistically robust result favours the fact that a high proportion of inclusions are actually monomineralic. This is better accounted for if microcrystals formed in the hybrid melt, likely in response of the early stage of the out of equilibrium hybridization process, then were eventually entrapped, mostly as single crystals, during the skeletal growth of chromite (Prichard et al., 2015), consistent with the square to rounded shape of the inclusions (Fig. 2a-b).

In this frame, the amphibole and clinopyroxene that are almost the only minerals observed in inclusion in chromites in pure dunites may represent microcrystals formed during the early stage of hybridization between the MORB and the silica- and water-rich component before the system and the hybrid fluid/melt progressed into a more evolved stage (i.e. more advanced hybridized stage), crystallizing together the more diversified inclusions, chromite and other impregnation minerals upsection (e.g., Rospabé et al., 2018; 2019a).

Since similar inclusions were observed in more concentrated chromitite ore bodies from the Maqsad area (Lorand and Ceuleneer, 1989; Leblanc and Ceuleneer, 1991; Borisova et al., 2012; Rollinson et al., 2018; Zagrtdenov et al., 2018; Rospabé et al., 2019b; Yao et al., 2020), it is likely that the same mantle dunitization process drove the formation of both the dunites and chromitites. The very details of the dunite-chromitite association remain unclear at this stage and this assumption should be investigated further by a more statistical study of the silicate inclusions at the scale of the whole DTZ.

Structural control on the nature of the fluids-melts that formed the DTZ dunites

In our previous study we have reported on the remarkable petrological and geochemical variability along the cross-section studied here in details for its inclusions content (cross-section #3 in Rospabé et al., 2019a). Its lithological stratigraphy (Fig. 1) is consistent with what is observed at the scale of the whole Maqsad DTZ (Rospabé, 2018). The vertical distribution of the silicate inclusions, roughly consistent with the whole rocks and matrix minerals major and trace elements trends, was suspected but needed to be confirmed with a higher analysis density, and the bearing of these variations on the DTZ genesis can now be discussed with an improved degree of confidence.

In addition to the statements discussed above about the nature of the inclusions, the main facts highlighted in this study are:

i) the abundance of inclusions in a given sample depends on the host lithology, being globally more abundant in pure dunites in the lower part of the cross-section and decreasing upsection within the impregnated interval (Fig. 1c);
ii) the abundance of silicate inclusions in disseminated chromites locally varies in a coherent way relative to the distribution of fault zones (Fig. 1c), reminiscent to the relation observed between the local higher inclusions content and the presence of magmatic breccias along the stratiform chromitite located about 1.5 km to the SE of the present cross-section (Rospabé et al., 2019b).

In terms of chemical compositions, it can then be observed that:

i) vertical evolutions are not random, with successive and alternating trends in most species (Fig. 4), reminiscent to what was already described in the composition of both the dunitic matrix and impregnating minerals of the Maqsad DTZ (Rospabé et al., 2018);
ii) the vertical chemical evolutions are conditioned by the proximity to the fault zones similarly to the composition of the host dunites (Rospabé et al., 2019a), including for elements considered as immobile during alteration such as the TiO_2 content;
iii) approaching fault zones, amphibole in inclusion (the most common phase with clinopyroxene, Fig. 1), is progressively enriched in K (lower Na#), P_2O_5, F and Cl (Fig. 4b).

The faults and fractures we mapped within the DTZ look to post-date the magmatic activity if only referring to the alteration mineralogy within fracture planes affecting the host dunite (dominated by serpentine and, in a lesser extent, carbonates). Similarly, faults within the lower crustal section of the Oman ophiolite were described for their role in the important hydrothermal alteration of the layered gabbros (Zihlmann et al., 2018). On the other hand, strong arguments were provided for the development of higher temperature, syn-magmatic fault zones in the vicinity of the Maqsad area. A N130°E-oriented fault system, parallel to the spreading axis that developed above the Maqsad diapir (Pallister, 1981; Ceuleneer, 1991; MacLeod and Rothery, 1992), was active at high temperature, early enough during the accretion of the oceanic lithosphere to have disturbed the crystallization of gabbros at the base of the crust (i.e. buffering of the An content in plagioclase to unusual high values, occurrence of Ti-rich pegmatitic gabbros; Abily et al., 2011).

Similarly, the fact that, i) the vertical chemical evolutions of the inclusions are progressive and continuous along the DTZ, over intervals having a characteristic thickness of about 50 m (Fig. 4) (i.e. not abruptly shifted by the faults), and that, ii) it concerns elements for which variations in concentration call for igneous processes such as Ti (in whole rocks, mineral impregnations, chromite, and silicate inclusions), confirms that syn-magmatic faults or fractures developed early within the dunitic mantle-crust transition zone, strongly influenced the nature of the different melt and/or fluid fractions percolating through the DTZ and played an important role on the mobilization of Cr at the mantle-crust transition (Rospabé et al., 2019a).

The higher concentration in phosphorous and halogens, especially Cl, in amphibole inclusions approaching fault zones supports the seawater-derived origin of the fluid fraction involved in the genesis of hybrid melts within the DTZ. This confirms the potential role of fault zones both for extraction of melts and introduction of high temperature hydrothermal fluids (i.e. they make possible the hybridization process, Rospabé et al., 2019a; 2019b). Then, at the time of the hybridization the hydrated component/MORB ratio was higher within fault zones than within the massive dunitic levels, as also attested by the lower TiO_2 toward the faults (Fig. 4).

Otherwise, the circulation of very saline fluids (brine-type) and subsequent hydrothermal fluid-rock reaction was documented by the discovery of Cl-rich amphiboles (0.1-5 wt%) in gabbros from the deep lower oceanic crust of the Wadi Tayin

massif, Oman (Currin et al., 2018a; 2018b). In this way, the Cl-apatite we observed along the cross-section may potentially result from a magmatic to metamorphic process involving such high temperature hydrothermal fluids following the cessation of the magmatic activity in a cooling system.

Another observation is that the abundance of inclusions spatially varies, partly in relation with the presence of faults or fractures (Fig. 1c): higher inclusion contents are roughly observed within the un-faulted dunitic levels, and especially within the chromite-rich interval ~ 750-775 m in altitude, rather than close to the faults (excepting in the lower impregnated level), as opposed to the inclusion distribution relative to magmatic breccias (i.e. frozen stages of fault development) along the neighbouring stratiform chromitite (Rospabé et al., 2019b). This distribution can reflect, i) better favoured conditions for the nucleation of the microcrystals within un-faulted levels where the contribution of the MORB is higher or, ii) a faster/earlier formation of the chromite grains relative to the microcrystals close to the faults where the contribution of the hydrated component is higher, or both, preventing significant entrapment of microcrystals. At the scale of the DTZ as a whole, the higher abundance of inclusions in dispersed chromites in pure dunites than in impregnated ones (Fig. 1c) may result from the local thermal state as pure dunite are supposed to have been compacted at higher temperature (i.e. above the crystallization temperature of the interstitial impregnation; Rospabé et al., 2018), the inclusions being the solely crystallization products with chromite in the deeper levels of the DTZ while fractionation from the percolating fluids/melts is also expressed in the impregnations in the shallower levels. This highlights that within the dunitic transition zone, in spite some features are shared between the formation of both dunite and chromitite, local differences may affect the formation and entrapment conditions of the silicate inclusions in chromite grains. It may reflect the competition between the crystallization of those exotic phases and the massive precipitation of chromite.

CONCLUSIONS

In the DTZ, the inclusion content in the dispersed chromites remarkably correlates with mineral impregnations in the host dunites, both in term of nature and chemical composition. This result first demonstrates that the inclusions in chromite, at least in the case we studied, are not the preserved relics of previous igneous events that happened in a totally different setting (e.g., high pressure processes in the deep mantle), then highlights the need of considering the census and analysis of inclusions in chromite in the systematic survey of the DTZ, in addition to the matrix minerals, to progress in the understanding of the fluid-melt-rock reactions occurring at Moho level below oceanic spreading centres. The development of synmagmatic faults at the mantle-crust transition is proposed, i) to occur as early as the dunitization stage implying the re-mobilization of Cr and other elements, ii) to condition the fluid-melt hybridization and fluid-melt-rock reactions in the shallow mantle and, potentially, iii) to strongly impact our views concerning the budget of many elements in oceanic spreading settings and the calculation of the global transfers between the mantle, crust and hydrosphere according to deep fluid circulation and hybrid melts genesis. Considering the specific case of halogens, our study suggests that they could be mobilized at very high temperature and not only during low temperature alteration processes (e.g., Kendrick et al., 2015; Chavrit et al., 2016; Kendrick et al., 2017; Kendrick, 2019).

ACKNOWLEDGMENTS

We gratefully thank F. de Parseval and J.-F. Ména for thin sections realization and J. Langlade for assistance with the EPMA analyses. We are grateful to M. Al Araimi, M. Al Batashi, A. Al-Rajhi, S. Almusharrafi and other colleagues from the Ministry of Commerce and Industry, Sultanate of Oman, as well as H. Al Azri, for their constant hospitality. We are grateful to S. Arai and Q. Xiong for their suggestions and very constructive comments as well as to C.-Z. Liu and A. Montanini for editorial handling. This work has been financially supported by the Centre National de la Recherche Scientifique-Institut National des Sciences de l'Univers (CNRS-INSU).

Supplementary data to this article are available online at https://doi.org/10.4454/ofioliti.v45i2.534

REFERENCES

Abily B., 2011. Caractéristiques pétrographique, géochimique et structurale de la section crustale profonde de l'ophiolite d'Oman : implications pour la genèse des magmas et le fonctionnement des chambres magmatiques à l'aplomb d'un centre d'expansion océanique. Univ. Paul Sabatier, Toulouse III.

Abily B. and Ceuleneer G., 2013. The dunitic mantle-crust transition zone in the Oman ophiolite: Residue of melt-rock interaction, cumulates from high-mgo melts, or both? Geology, 41: 67-70, doi: 10.1130/G33351.1.

Abily B., Ceuleneer G. and Launeau P., 2011. Synmagmatic normal faulting in the lower oceanic crust: Evidence from the Oman ophiolite. Geology, 39: 391-394, doi: 10.1130/G31652.1.

Amri I., Benoit M. and Ceuleneer G., 1996. Tectonic setting for the genesis of oceanic plagiogranites: evidence from a paleospreading structure in the Oman ophiolite. Earth Planet. Sci. Lett., 139: 177-194, doi: 10.1016/0012-821X(95)00233-3.

Arai S., 1998. Comments of the paper "Primitive basaltic melts included in podiform chromites from the Oman ophiolite" by P. Schiano et al. Earth Planet. Sci. Lett., 156: 117-119, doi: 10.1016/S0012-821X(97)00210-0.

Benn K., Nicolas A. and Reuber I., 1988. Mantle-crust transition zone and origin of wehrlitic magmas: Evidence from the Oman ophiolite. Tectonophysics, 151: 75-85, doi: 10.1016/0040-1951(88)90241-7.

Benoit M., Ceuleneer G. and Polvé M., 1999. The remelting of hydrothermally altered peridotite at mid-ocean ridges by intruding mantle diapirs. Nature, 402: 514-518, doi: 10.1038/990073.

Benoit M., Polvé M. and Ceuleneer G., 1996. Trace element and isotopic characterization of mafic cumulates in a fossil mantle diapir (Oman ophiolite). Chem. Geol., 134: 199-214, doi: 10.1016/S0009-2541(96)00087-3.

Borisova A.Y., Ceuleneer G., Kamenetsky V.S., Arai S., Béjina F., Abily B., Bindeman I.N., Polvé M., De Parseval P., Aigouy T. and Pokrovski G.S., 2012. A new view on the petrogenesis of the Oman ophiolite chromitites from microanalyses of chromite-hosted inclusions. J. Petrol., 53: 2411-2440, doi: 10.1093/petrology/egs054.

Boudier F. and Al-Rajhi A., 2014. Structural control on chromitite deposits in ophiolites: The oman case. Geol. Soc. London Spec. Publ., 392: 263-277, doi: 10.1144/SP392.14.

Boudier F. and Nicolas A., 1995. Nature of the moho transition zone in the Oman ophiolite. J. Petrol., 36: 777-796, doi: 10.1093/petrology/36.3.777.

Boudier F., Ceuleneer G. and Nicolas A., 1988. Shear zones, thrusts and related magmatism in the Oman ophiolite: Initiation of thrusting on an oceanic ridge. Tectonophysics, 151: 275-296, doi: 10.1016/0040-1951(88)90249-1.

Ceuleneer G., 1991. Evidence for a Paleo-Spreading Center in the Oman Ophiolite: Mantle Structures in the Maqsad Area. In: Tj. Peters, A. Nicolas and R.G. Coleman (Eds.), Ophiolite genesis and evolution of the oceanic lithosphere, Springer, Dordrecht, p. 147-173, doi: 10.1007/978-94-011-3358-6_9.

Ceuleneer G. and Nicolas A., 1985. Structures in podiform chromite from the Maqsad district (Sumail ophiolite, Oman). Miner. Depos., 20: 177-184, doi: 10.1007/BF00204562

Ceuleneer G., Monnereau M. and Amri I., 1996. Thermal structure of a fossil mantle diapir inferred from the distribution of mafic cumulates. Nature, 379: 149-153, doi: 10.1038/379149a0.

Ceuleneer G., Nicolas A. and Boudier F., 1988. Mantle flow patterns at an oceanic spreading centre: The Oman peridotites record. Tectonophysics, 151: 1-26, doi: 10.1016/0040-1951(88)90238-7.

Chavrit D., Burgess R., Sumino H., Teagle D.A.H., Droop G., Shimizu A. and Ballentine C.J., 2016. The contribution of hydrothermally altered ocean crust to the mantle halogen and noble gas cycles. Geochim. Cosmochim. Acta., 183: 106-124, doi:10.1016/j.gca.2016.03.014.

Clénet H., Ceuleneer G., Pinet P., Abily B., Daydou Y., Harris E., Amri I. and Dantas C., 2010. Thick sections of layered ultramafic cumulates in the Oman ophiolite revealed by an airborne hyperspectral survey: Petrogenesis and relationship to mantle diapirism. Lithos, 114: 265-281, doi: 10.1016/j.lithos.2009.09.002.

Constantin, M., 1999. Gabbroic intrusions and magmatic metasomatism in harzburgites from the Garrett transform fault: implications for the nature of the mantle-crust transition at fast-spreading ridges. Contrib. Miner. Petrol., 136: 111-130, doi: 10.1007/s004100050527.

Currin A., Koepke J., Almeev R.R. and Beermann O., 2018b. Interaction of highly saline fluid and olivine gabbro: Experimental simulation of deep hydrothermal processes involving amphibole at the base of the oceanic crust. Lithos, 323: 91-102, doi: 10.1016/j.lithos.2018.09.017.

Currin A., Wolff P.E., Koepke J., Almeev R.R., Zhang C., Zihlmann B., Ildefonse B. and Teagle D.A.H., 2018a. Chlorine-rich amphibole in deep layered gabbros as evidence for brine/ rock interaction in the lower oceanic crust: A case study from the Wadi Wariyah, Samail Ophiolite, Sultanate of Oman. Lithos, 323: 125-136, doi: 10.1016/j.lithos.2018.09.015.

Dick H.J.B., 1977. Evidence of partial melting in the Josephine peridotite. Oregon Dept. Geol. Miner. Ind. Bull., 96: 59-62.

Glennie K.W., Boeuf M.G.A., Clarke M.H., Moody-Stuart M., Pilaar W.F.H. and Reinhardt B.M., 1973. Late Cretaceous nappes in Oman Mountains and their geologic evolution. Am. Assoc. Pet. Geol. Bull., 57: 5-27, doi: 10.1306/819A4240-16C5-11D7-8645000102C1865D.

Godard M., Jousselin D. and Bodinier J.-L., 2000. Relationships between geochemistry and structure beneath a palaeo-spreading centre: A study of the mantle section in the Oman ophiolite. Earth Planet. Sci. Lett., 180: 133-148, doi: 10.1016/S0012-821X(00)00149-7.

Johan Z., Dunlop H., Le Bel L., Robert J.L. and Volfinger M., 1983. Origin of chromite deposits in ophiolitic complexes: evidence for a volatile- and sodium-rich reducing fluid phase. Fortschr. Miner., 61: 105-107.

Johan Z., Martin R.F. and Ettler V., 2017. Fluids are bound to be involved in the formation of ophiolitic chromite deposits. Eur. J. Miner., 29: 543-555, doi: 10.1127/ejm/2017/0029-2648.

Jousselin D., Nicolas A. and Boudier F., 1998. Detailed mapping of a mantle diapir below a paleo-spreading center in the Oman ophiolite. J. Geophys. Res. Solid Earth, 103: 18153-18170, doi: 10.1029/98JB01493.

Kelemen P.B., 1990. Reaction between ultramafic rock and fractionating basaltic magma I. phase relations, the origin of calc-alkaline magma series, and the formation of discordant dunite. J. Petrol., 31: 51-98, doi: 10.1093/petrology/31.1.51.

Kelemen P.B., Dick H.J.B. and Quick J.E., 1992. Formation of harzburgite by pervasive melt/rock reaction in the upper mantle. Nature, 358: 635-641, doi: 10.1038/358635a0.

Kelemen P.B., Koga K. and Shimizu N., 1997. Geochemistry of gabbro sills in the crust-mantle transition zone of the Oman ophiolite: implications for the origin of the oceanic lower crust. Earth Planet. Sci. Lett., 146: 475-488, doi: 10.1016/S0012-821X(96)00235-X.

Kelemen P.B., Shimizu N. and Salters V.J.M., 1995. Extraction of mid-ocean-ridge basalt from the upwelling mantle by focused flow of melt in dunite channels. Nature, 375: 747-753, doi: 10.1038/375747a0.

Kendrick M.A., 2019. Halogens in altered ocean crust from the East Pacific Rise (ODP/IODP Hole 1256D). Geochim. Cosmochim. Acta, 261: 93-112, doi: 10.1016/J.GCA.2019.06.044.

Kendrick M.A., Hémond C., Kamenetsky V.S., Danyushevsky L., Devey C.W., Rodemann T., Jackson M.G. and Perfit M.R., 2017. Seawater cycled throughout Earth's mantle in partially serpentinized lithosphere. Nat. Geosci., 10: 222-228, doi: 10.1038/ngeo2902.

Kendrick M.A., Honda M. and Vanko D.A., 2015. Halogens and noble gases in Mathematician Ridge meta-gabbros, NE Pacific: implications for oceanic hydrothermal root zones and global volatile cycles. Contrib. Miner. Petrol., 170: 43, doi: 10.1007/s00410-015-1192-x.

Koga K.T., Kelemen P.B. and Shimizu N., 2001. Petrogenesis of the crust-mantle transition zone and the origin of lower crustal wehrlite in the Oman ophiolite. Geochemistry, Geophys. Geosystems, 2, doi: 10.1029/2000GC000132.

Korenaga J. and Kelemen P.B., 1997. Origin of gabbro sills in the Moho transition zone of the Oman ophiolite: Implications for magma transport in the oceanic lower crust. J. Geophys. Res. Solid Earth, 102: 27729-27749, doi: 10.1029/97JB02604.

Leblanc M. and Ceuleneer G., 1991. Chromite crystallization in a multicellular magma flow: Evidence from a chromitite dike in the Oman ophiolite. Lithos, 27: 231-257, doi: 10.1016/0024-4937(91)90002-3.

Lorand J.P. and Ceuleneer G., 1989. Silicate and base-metal sulfide inclusions in chromites from the Maqsad area (Oman ophiolite, Gulf of Oman): A model for entrapment. Lithos, 22: 173-190, doi: 10.1016/0024-4937(89)90054-6.

MacLeod C.J. and Rothery D.A., 1992. Ridge axial segmentation in the Oman ophiolite: Evidence from along-strike variations in the sheeted dyke complex. Geol. Soc. London Spec. Publ., 60: 39-63, doi: 10.1144/GSL.SP.1992.060.01.03.

Matveev S. and Ballhaus C., 2002. Role of water in the origin of podiform chromitite deposits. Earth Planet. Sci. Lett., 203: 235-243. doi: 10.1016/S0012-821X(02)00860-9.

Montigny R., Le Mer O., Thuizat R. and Whitechurch H., 1988. K-Ar and Ar study of metamorphic rocks associated with the Oman ophiolite: Tectonic implications. Tectonophysics, 151: 345-362, doi: 10.1016/0040-1951(88)90252-1.

Pallister J.S., 1981. Structure of the sheeted dike complex of the Samail Ophiolite near Ibra, Oman. J. Geophys. Res. Solid Earth, 86: 2661-2672, doi: 10.1029/JB086iB04p02661.

Prichard H.M., Barnes S.J., Godel B., Reddy S.M., Vukmanovic Z., Halfpenny A., Neary C.R. and Fisher P.C., 2015. The structure of and origin of nodular chromite from the Troodos ophiolite, Cyprus, revealed using high-resolution X-ray computed tomography and electron backscatter diffraction. Lithos, 218-219: 87-98, doi: 10.1016/j.lithos.2015.01.013.

Python M. and Ceuleneer G., 2003. Nature and distribution of dykes and related melt migration structures in the mantle section of the Oman ophiolite. Geochem., Geophys. Geosyst., 4, doi: 10.1029/2002GC000354.

Python M., Ceuleneer G. and Arai S., 2008. Chromian spinels in mafic-ultramafic mantle dykes: Evidence for a two-stage melt production during the evolution of the Oman ophiolite. Lithos, 106: 137-154, doi: 10.1016/j.lithos.2008.07.001.

Python M., Ceuleneer G., Ishida Y., Barrat J.-A., Arai S., 2007a. Oman diopsidites: a new lithology diagnostic of very high temperature hydrothermal circulation in mantle peridotite below oceanic spreading centres. Earth Planet. Sci. Lett., 255: 289-305, doi: 10.1016/j.epsl.2006.12.030.

Python M., Ishida Y., Ceuleneer G. and Arai S., 2007b. Trace element heterogeneity in hydrothermal diopside: evidence for Ti depletion and Sr-Eu-LREE enrichment during hydrothermal metamorphism of mantle harzburgite. J. Miner. Petrol. Sci., 102: 143-149, doi: 10.2465/jmps.060830.

Python M., Yoshikawa M., Shibata T. and Arai S., 2011. Diopsidites and rodingites: serpentinisation and Ca-metasomatism in the Oman ophiolite mantle. In: R.K. Srivastava (Ed.), Dyke swarms: Keys for geodynamic interpretation, Springer, Berlin, Heidelberg, p. 401-435. doi: 10.1007/978-3-642-12496-9_23.

Quick J.E., 1981. The origin and significance of large, tabular dunite bodies in the Trinity peridotite, northern California. Contrib. Miner. Petrol., 78: 413-422, doi: 10.1007/BF00375203.

Rabinowicz M., Ceuleneer G. and Nicolas A., 1987. Melt segregation and flow in mantle diapirs below spreading centers: evidence from the Oman ophiolite. J. Geophys. Res. Solid Earth, 92: 3475-3486, doi: 10.1029/JB092iB05p03475.

Rioux M., Bowring S., Kelemen P., Gordon S., Miller R. and Dudás F., 2013. Tectonic development of the Samail ophiolite: High-precision U-Pb zircon geochronology and Sm-Nd isotopic constraints on crustal growth and emplacement. J. Geophys. Res. Solid Earth, 118: 2085-2101, doi: 10.1002/jgrb.50139.

Rioux M., Garber J., Bauer A., Bowring S., Searle M., Kelemen P. and Hacker B., 2016. Synchronous formation of the metamorphic sole and igneous crust of the Semail ophiolite: New constraints on the tectonic evolution during ophiolite formation from high-precision U-Pb zircon geochronology. Earth Planet. Sci. Lett., 451: 185-195, doi: 10.1016/j.epsl.2016.06.051.

Rollinson H. and Adetunji J., 2013. Mantle podiform chromitites do not form beneath mid-ocean ridges: A case study from the Moho transition zone of the Oman ophiolite. Lithos, 177: 314-327, doi: 10.1016/j.lithos.2013.07.004.

Rollinson H., Mameri L. and Barry T., 2018. Polymineralic inclusions in mantle chromitites from the Oman ophiolite indicate a highly magnesian parental melt. Lithos, 310-311: 381-391, doi: 10.1016/j.lithos.2018.04.024.

Rospabé M., 2018. Etude pétrologique, géochimique et structurale de la zone de transition dunitique dans l'ophiolite d'Oman : Identification des processus pétrogénétiques à l'interface manteau/croûte. Univ. Paul Sabatier, Toulouse III.

Rospabé M., Benoit M., Ceuleneer G., Hodel F. and Kaczmarek M.-A., 2018. Extreme geochemical variability through the dunitic transition zone of the Oman ophiolite: Implications for melt/fluid-rock reactions at Moho level beneath oceanic spreading centers. Geochim. Cosmochim. Acta, 234: 1-23, doi: 10.1016/j.gca.2018.05.012.

Rospabé M., Benoit M., Ceuleneer G., Kaczmarek M.-A. and Hodel F., 2019a. Melt hybridization and metasomatism triggered by syn-magmatic faults within the Oman ophiolite: A clue to understand the genesis of the dunitic mantle-crust transition zone. Earth Planet. Sci. Lett., 516: 108-121, doi: 10.1016/j.epsl.2019.04.004.

Rospabé M., Ceuleneer G., Benoit M., Abily B. and Pinet P., 2017. Origin of the dunitic mantle-crust transition zone in the Oman ophiolite: The interplay between percolating magmas and high-temperature hydrous fluids. Geology, 45: 471-474, doi: 10.1130/G38778.1.

Rospabé M., Ceuleneer G., Granier N., Arai S. and Borisova A.Y., 2019b. Multi-scale development of a stratiform chromite ore body at the base of the dunitic mantle-crust transition zone (Maqsad diapir, Oman ophiolite): The role of repeated melt and fluid influxes. Lithos, 350: 105235, doi: 10.1016/j.lithos.2019.105235.

Sanfilippo A., Morishita T. and Senda R., 2016. Rhenium-osmium isotope fractionation at the oceanic crust-mantle boundary. Geology, 44: 167-170, doi:10.1130/G37428.1.

Sanfilippo A., Tribuzio R. and Tiepolo M., 2014. Mantle-crust interactions in the oceanic lithosphere: Constraints from minor and trace elements in olivine. Geochim. Cosmochim. Acta, 141: 423-439, doi:10.1016/j.gca.2014.06.012.

Schiano P., Clocchiatti R., Lorand J.P., Massare D., Deloule E. and Chaussidon M., 1997. Primitive basaltic melts included in podiform chromites from the Oman Ophiolite. Earth Planet. Sci. Lett., 146: 489-497, doi: 10.1016/s0012-821x(96)00254-3.

Talkington R.W., Watkinson D.H., Whittaker P.J. and Jones P.C., 1984. Platinum-group minerals and other solid inclusions in chromite of ophiolitic complexes: Occurrence and petrological significance. Tscherm. Miner. Petrogr. Mitt., 32: 285-301, doi: 10.1007/BF01081619.

Warren C.J., Parrish R.R., Waters D.J. and Searle M.P., 2005. Dating the geologic history of Oman's Semail ophiolite: Insights from U-Pb geochronology. Contrib. Mineral. Petrol., 150: 403-422, doi: 10.1007/s00410-005-0028-5.

Yao Y., Takazawa E., Chatterjee S., Richard A., Morlot C., Créon L. Al-Busaidi S. and Michibayashi K., 2020. High resolution X-ray computed tomography and scanning electron microscopy studies of multiphase solid inclusions in Oman podiform chromitite: implications for post-entrapment modification. J. Miner. Petrol. Sci., 115: 247-260, doi: 10.2465/jmps.191008.

Zagrtdenov N.R., Ceuleneer G., Rospabé M., Borisova A.Y., Toplis M.J., Benoit M. and Abily B., 2018. Anatomy of a chromitite dyke in the mantle/crust transition zone of the Oman ophiolite. Lithos, 312: 343-357, doi: 10.1016/j.lithos.2018.05.012.

Zihlmann B., Müller S., Coggon R.M., Koepke J., Garbe-Schönberg D. and Teagle D.A.H., 2018. Hydrothermal fault zones in the lower oceanic crust: An example from Wadi Gideah, Samail ophiolite, Oman. Lithos, 303: 103-124, doi: 10.1016/j.lithos.2018.09.008.

Received, March 9, 2020
Accepted, April 21, 2020